$\mathcal{R}$-matrix theory of driven electromagnetic cavities

F. Beck,* C. Dembowski,† A. Heine,‡ and A. Richter§
Institut für Kernphysik, Technische Universität Darmstadt, D-64289 Darmstadt, Germany
(Received 4 September 2002; revised manuscript received 7 January 2003; published 17 June 2003)

The resonances of cylindrical symmetric microwave cavities are analyzed in $\mathcal{R}$-matrix theory, which transforms the input channel conditions to the output channels. Single and interfering double resonances are studied and compared with experimental results obtained with superconducting microwave cavities. Because of the equivalence of the two-dimensional Helmholtz and the stationary Schrödinger equations, the results give insight into the resonance structure of regular and chaotic quantum billiards.

DOI: 10.1103/PhysRevE.67.066208 PACS number(s): 05.45.Mt, 41.20.Jb, 25.70.Ef

I. INTRODUCTION

Nuclear reactions at low energies are characterized by narrow resonances which, in the case of well separated resonances, show a Breit-Wigner shape. If the separation is small, however, interference occurs, which can lead to complicated nonhomogeneous resonance shapes. This was already observed in the early days of the study of slow neutron resonances. These data stimulated the theoretical development of resonance theories, such as, e.g., the stationary $\mathcal{R}$-matrix theory of Wigner and Eisenbud [1], or the equivalent one for running waves of Kapur and Peierls [2]. The idea behind this work is a transformation from the input to the output channels without taking into account explicitly the complex dynamics of the strongly interacting system, which enters only through the parameters of the transformation matrix. These parameters have to be obtained by fitting the resulting multichannel cross section to experimental data. The essential benefit of the Wigner and Eisenbud formulation is the transformation to standing waves, which results in a spatially stationary problem with real boundary conditions rather than the complex boundary conditions of running waves in each channel. Nevertheless, this procedure gets rather complicated when more than one resonance contributes significantly, and empirical analysis can be hindered considerably by insufficient statistics and large background contributions. A complete representation of the theoretical as well as the practical aspects of $\mathcal{R}$-matrix theory in nuclear physics which constituted the basis for the widespread later work in this field is the review article of Lane and Thomas [3]. Although in a different context from the present paper, $\mathcal{R}$-matrix theory has also recently been applied to multiphoton processes [4,5], in the analysis of Rydberg spectra [6,7], and to chaotic ionization of Rydberg states [8,9].

A sensitive test of single- and multilevel resonance theories can be obtained in the electromagnetic analog of a quantum mechanical multichannel system in the form of a flat superconducting cavity, fed with microwave radiation [10,11]. It has been shown [10] that all resonances of such a system can be resolved and analyzed with respect to their positions and widths. This allows a clean verification of level statistics for regular and chaotic cavities, respectively, depending on the geometrical shape of the flat resonator. Superconducting cavities, with their high quality factors, can, however, also be analyzed with respect to the line shapes of isolated and overlapping resonances, which are almost undisturbed by additional broadening from wall losses leading to strongly overlapping resonances in the spectra, as in normal conducting resonators. This is typically true in the high frequency part of the spectra, relevant especially for chaotic systems [11]. There, the ''true'' resonances, i.e., not additionally broadened, still have widths smaller than the mean level distance, which allows a theoretical approach on the basis of groups of isolated resonances. Analyses of resonances with the Breit-Wigner formula were performed in [12,13]. We amend this work in two respects. First, we start from the electromagnetic field conditions of microwave cavities, rather than assuming the Breit-Wigner formula as valid there also, and, second, we use the $\mathcal{R}$-matrix formalism, rather than starting directly with the S matrix, since the parameters of the $\mathcal{R}$ matrix allow direct modeling of resonance shapes and comparison of resonances in different channels.

In this paper, we first derive the resonance theory of a two-dimensional microwave cavity, following the idea of Wigner and Eisenbud [1] to parametrize the relation between input and output in the form of a multilevel reactance matrix. From this, the S matrix, giving the power transfer from input to output, can be constructed by a nonlinear transformation which leads, in the multilevel case, to rather involved interference structures.

The approach is tested with the experimentally determined single and double resonances of a superconducting two-dimensional billiard of threefold (C_3) symmetry [14,15]. We also analyze the single resonances of a three-dimensional stadium billiard [16]. The tests are performed in the low as well as in the high frequency parts of the spectra, in order to cover, on one hand, strong resonances which extend over several orders of magnitude, and, on the other hand, the relevant frequency part for analyzing the dynamics of the system. At high frequencies level interference occurs, leading to characteristic nonuniform line shapes. Comparing our one-level formula with the Breit-Wigner formula of nuclear physics shows that for narrow and isolated resonances the difference is negligibly small.

*Electronic address: freder.beck@physik.tu-darmstadt.de
†Electronic address: dembowski@ikp.tu-darmstadt.de
‡Electronic address: heine@ikp.tu-darmstadt.de
§Electronic address: richter@ikp.tu-darmstadt.de

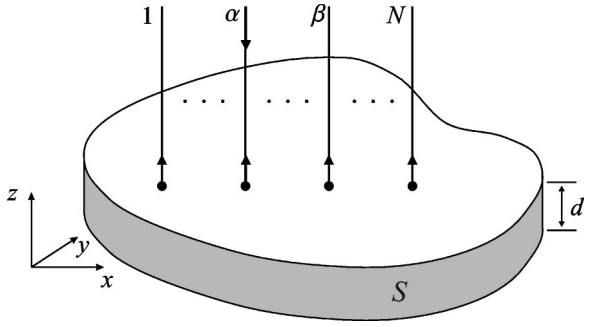

FIG. 1. Sketch of the flat cavity with N connecting antennas. The feeding antenna is denoted by α; d, height of the cylindrical cavity, closed with two parallel plates perpendicular to the cylinder; S, cylinder surface; z is the longitudinal and $\{x,y\}$ are the transverse coordinates.

II. DERIVATION OF THE CAVITY RESONANCE FORMULA

A. The cavity and antenna wave functions

We treat a cylindrical microwave cavity with N antennas $1,\ldots,\alpha,\ldots,\beta,\ldots,N$ connected perpendicular to it. One antenna, which we always denote by α, is feeding the cavity while radiation is extracted through the others (multichannel situation; see Fig. 1). The electromagnetic fields in the cavity can be derived from scalar fields [17], and it suffices to treat these. The complete scalar wave function with fixed frequency ω can be written as

$$\Xi(\vec{r},t)=\Psi(\vec{r})\exp(-i\omega t), \quad \vec{r}=\{x,y,z\}, \tag{1}$$

with the spatial part $\Psi(\vec{r})$ obeying the wave equation

$$\left(\Delta+\frac{\omega^2}{c^2}\right)\Psi(\vec{r})=0. \tag{2}$$

For a cavity with arbitrary cross-sectional shape, but with end plates perpendicular to the cylinder (cf. Fig. 1), the spatial part $\Psi(\vec{r})$ can be separated into longitudinal and transverse components, according to $\Psi(\vec{r})=\psi(z)\chi(\vec{r}_t)$ with z the longitudinal and $\vec{r}_t=x\cdot\vec{e}_1+y\cdot\vec{e}_2$ the transverse coordinates. The z-dependent part consists of standing waves $A\sin kz+B\cos kz$, and the boundary conditions $\vec{E}_t=\vec{0}$ at $z=0$ and $z=d$ for transverse magnetic (TM) fields lead with $k=p\pi/d$ to the form

$$E_z=\psi_{TM,p}(z)\chi(x,y)=\cos\left(\frac{p\pi z}{d}\right)\chi(x,y), \quad p=0,1,2,\ldots, \tag{3}$$

while for transverse electric (TE) fields the vanishing of H_z at the z boundaries requires

$$H_z=\psi_{TE,p}(z)\chi(x,y)=\sin\left(\frac{p\pi z}{d}\right)\chi(x,y), \quad p=1,2,3,\ldots. \tag{4}$$

For flat cavities, i.e., d much smaller than the wavelength of the resonating microwaves in the cavity, TM modes are the only possible ones since the $p=0$ modes alone can exist. This is the interesting case for a comparison with quantum mechanics [11]. However, the following derivation is more general and holds for any value of p, thus describing arbitrary cavities with cylindrical geometry. The transverse part $\chi(\vec{r})$ is a solution of the two-dimensional wave equation

$$\left(\Delta_t+\frac{\omega_p^2}{c^2}\right)\chi_p(\vec{r}_t)=0, \quad \Delta_t\equiv\Delta-\frac{\partial^2}{\partial z^2}, \quad \omega_p^2=\omega^2-\left(\frac{cp\pi}{d}\right)^2 \tag{5}$$

with the boundary condition on the cylindrical surface S (cf. Fig. 1)

$$\chi_p|_S=0. \tag{6}$$

Equation (5) together with Eq. (6) defines an eigenvalue problem for the two-dimensional transverse fields with eigenfunctions $\chi_{pr}(\vec{r}_t)$, $r=1,2,3,\ldots$. For $p=0$, these fields are the direct analog of the stationary wave functions of a two-dimensional quantum billiard which makes the study of the flat electromagnetic cavity interesting for illuminating the implications of quantum chaos. The TM fields are given by

$$\vec{E}_t=-\frac{p\pi c^2}{d\omega_p^2}\sin\left(\frac{p\pi z}{d}\right)\vec{\nabla}_t\chi_{pr},$$

$$\vec{H}_t=\frac{i\omega c}{\omega_p^2}\cos\left(\frac{p\pi z}{d}\right)\vec{\nabla}_t\chi_{pr}.$$

The whole system can be divided geometrically into an *internal* and an *external* part, where the internal part consists of the cavity proper, while the external parts are the N antenna wave guides. The concept of the $\mathcal{R}$-matrix approach consists of obtaining a transformation from the feeding antenna to the output antennas by using the boundary conditions at the connections between internal and external regions.

The longitudinal wave in an arbitrary antenna μ out of the N antennas in general consists of incoming and outgoing parts

$$\psi_\mu(z_\mu)=A_\mu\exp(-ik_\mu z_\mu)+A'_\mu\exp(ik_\mu z_\mu).$$

The transverse part $\chi_\mu(\vec{r}_{\mu t})$ also obeys the reduced wave equation

$$\left(\Delta_{\mu t}+\frac{\omega_\mu^2}{c^2}\right)\chi_\mu(\vec{r}_{\mu t})=0, \quad \Delta_{\mu t}\equiv\Delta-\frac{\partial^2}{\partial z_\mu^2},$$

$$\omega_\mu^2=\omega^2-c^2k_\mu^2. \tag{7}$$

For the group velocity of the running wave in antenna μ one obtains

$$v_{g\mu}=\frac{d\omega}{dk_\mu}=\frac{c^2k_\mu}{\omega}. \tag{8}$$

We now specify to the case of N open antennas where the input into antenna α produces outgoing fluxes in α (direct reflection) as well as in all other antennas $\beta\neq\alpha$. For this purpose we introduce local antenna coordinates $\vec{r}_\mu$ for an arbitrary antenna μ according to

$$x_\mu=x-x_{\mu 0},\quad y_\mu=y-y_{\mu 0},\quad z_\mu=z-z_{\mu 0}$$

and $\{x_{\mu 0},y_{\mu 0},z_{\mu 0}\}$ denotes the footpoint of antenna μ. For the geometry of Fig. 1 we have $z_{\mu 0}=z_0=d$ for all N antennas. The spatial wave function $\Psi(\vec{r})$ depends on which of the N antennas has been chosen as the input antenna and thus contains incoming waves. For fixed frequency ω there are N such distinct wave functions which form a basis for the scalar cavity fields. To distinguish them they have to be marked by the index of the feeding antenna. With this notation the basis set consists of the N functions $\Psi_\mu(\vec{r})$, $\mu=1,\ldots,N$. With our convention, which always denotes the input channel by α, the spatial wave $\Psi_\alpha(\vec{r})$ approaches in antenna β of the external region the form

$$\Psi_\alpha(\vec{r}\to\vec{r}_\beta)=\psi_{\alpha\beta}(z_\beta)\chi_\beta(\vec{r}_{\beta t})\quad\text{in antenna }\beta. \tag{9}$$

Introducing the unitary S matrix that transforms input into output we can write the longitudinal parts in the form

$$\psi_{\alpha\beta}(z_\beta)=-S_{\alpha\beta}\exp(ik_\beta z_\beta)K_\beta,\quad \beta\neq\alpha,$$

$$\begin{aligned}\psi_{\alpha\alpha}(z_\alpha)&=[\exp(-ik_\alpha z_\alpha)-S_{\alpha\alpha}\exp(ik_\alpha z_\alpha)]K_\alpha\\&=(\psi_{in}+\psi_{out})K_\alpha,\end{aligned} \tag{10}$$

where K_β,K_α are normalizing constants. For later purposes it is convenient to choose normalizations such that the ingoing flux per unit time is normalized to 1, and the outgoing fluxes per unit time are given by the absolute squares of the S-matrix elements. This leads to

$$P_\alpha^{in}=K_\alpha^2\psi_{in}^*\psi_{in}\int\chi_\alpha^*\chi_\alpha d\sigma_\alpha v_{g\alpha}\overset{!}{=}1,\quad \int_\alpha\chi_\alpha^*\chi_\alpha d\sigma_\alpha\equiv f_\alpha,$$

$$K_\alpha=\frac{1}{(f_\alpha v_{g\alpha})^{1/2}}=\frac{1}{c}\left(\frac{\omega}{f_\alpha k_\alpha}\right)^{1/2}, \tag{11}$$

$$P_{\alpha\beta}^{out}=K_\beta^2|S_{\alpha\beta}|^2f_\beta v_{g\beta}\overset{!}{=}|S_{\alpha\beta}|^2,$$

$$K_\beta=\frac{1}{(f_\beta v_{g\beta})^{1/2}}=\frac{1}{c}\left(\frac{\omega}{f_\beta k_\beta}\right)^{1/2},$$

$$P_{\alpha\beta}^{out}=|S_{\alpha\beta}|^2\to P_{\alpha\beta}\equiv\frac{P_{\alpha\beta}^{out}}{P_\alpha^{in}}=|S_{\alpha\beta}|^2, \tag{12}$$

where α is the input antenna, $\beta\neq\alpha$ are the $N-1$ output antennas, and $d\sigma_\alpha$ is the transverse surface element in antenna α.

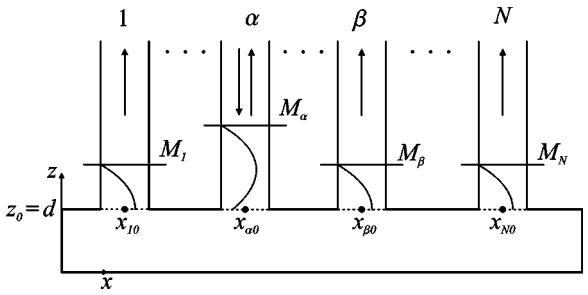

FIG. 2. Perpendicular cut through the cavity at the antenna entrances. To visualize the standing wave situation, virtual mirrors M_i are placed in the output antennas one-quarter wavelength away from the antenna footpoints in order to produce the boundary conditions as expressed in Eq. (16). In the input antenna the mirror M_α has to be placed at such a point that the frequency of the system stays at the continously varying value ω. This reflects itself in the presence of sine and cosine waves in the entrance channel, Eq. (15).

B. Transformation to standing waves

Analogous to the formalism of Wigner and Eisenbud [1] we perform a basis transformation to standing spatial waves $\Phi_\alpha(\vec{r})$, where the index α again indicates the input antenna, and the whole set $\{\Phi_\beta,\beta=1,\ldots,N\}$ is also complete for fixed ω. This has the benefit of rendering the boundary conditions real. Because of the completeness of both sets we can expand the function Φ_α into the set $\{\Psi_\beta\}$

$$\Phi_\alpha=\sum_\beta C_{\alpha\beta}\Psi_\beta. \tag{13}$$

In analogy to Eq. (9), the new base function $\Phi_\alpha(\vec{r})$ in the external region assumes the form

$$\Phi_\alpha(\vec{r}\to\vec{r}_\beta)=\phi_{\alpha\beta}(z_\beta)\chi_\beta(\vec{r}_{\beta t})\quad\text{in antenna }\beta \tag{14}$$

with

$$\phi_{\alpha\beta}(z_\beta)=\mathcal{R}_{\alpha\beta}\cos(k_\beta z_\beta)Z_\beta,\quad \beta\neq\alpha,$$

$$\phi_{\alpha\alpha}(z_\alpha)=[k_\alpha^{-1}\sin(k_\alpha z_\alpha)+\mathcal{R}_{\alpha\alpha}\cos(k_\alpha z_\alpha)]Z_\alpha, \tag{15}$$

where $\mathcal{R}$ is the derivative (Wigner and Eisenbud [1]) or reactance (as in most work on electromagnetic applications) matrix, and a factor k_α^{-1} has been put in for later convenience. From Eq. (15) follow the derivatives at the antenna footpoints

$$\left(\frac{d\phi_{\alpha\beta}}{dz_\beta}\right)\bigg|_0=0,\quad \left(\frac{d\phi_{\alpha\alpha}}{dz_\alpha}\right)\bigg|_0=Z_\alpha. \tag{16}$$

We can visualize this (see Fig. 2) by placing virtual mirrors (M_i) into the antenna waveguides such that the system becomes stationary with standing waves in each antenna. The mirror is located at all exit antennas a quarter wavelength away from the antenna footpoint, while in the feeding antenna it has to be placed in such a way that the frequency of the system assumes the freely choosable value ω.

Now, in the external region, we can identify the coefficients of the independent functions $\exp(ik_\mu z_\mu)$ and $\exp(-ik_\mu z_\mu)$ on both sides of Eq. (13) with the explicit forms of the wave functions in the external region, Eqs. (10) and (14), to arrive after a straightforward calculation at the connection between the $\mathcal{R}$ and S matrices, which in matrix notation reads

$$S=\rho(1-iB\mathcal{R}B)^{-1}(1+iB\mathcal{R}B)\rho \tag{17}$$

with the diagonal matrices

$$B_{\alpha\beta}=\delta_{\alpha\beta}k_\alpha^{1/2}, \quad \rho_{\alpha\beta}=\delta_{\alpha\beta}\exp(-ik_\alpha z_{\alpha 0}), \tag{18}$$

and with

$$Z_\mu=k_\mu^{1/2}K_\mu=\frac{1}{c}\left(\frac{\omega}{f_\mu}\right)^{1/2}. \tag{19}$$

Equation (17) defines the nonlinear relation between the S matrix and the reactance matrix $B\mathcal{R}B$.

C. Derivation of the reactance matrix

We now determine the reactance matrix from the relation between cavity eigenfunctions and antenna wave functions. This procedure is the essential part of the Wigner-Eisenbud approach, since it relates the S matrix Eq. (17) to the eigenstates of the cavity, without explicitly detailing its properties. We start with expanding the standing wave function Φ_α inside the cavity into the complete orthonormalized basis of cavity eigenfunctions Ψ_s, which are the cavity eigenstates when all antennas are removed (closed internal region)

$$\Phi_\alpha=\sum_s D_{\alpha s}\Psi_s, \tag{20}$$

and from Eqs. (3), (5), and (6) the set Ψ_s is defined (for transverse magnetic waves) by

$$\Psi_s(\vec{r})=\psi_{TM,p}(z)\chi_{pr}(x,y), \quad s\equiv\{p,r\}, \quad p=0,1,2,\ldots,$$
$$r=1,2,3,\ldots, \tag{21}$$

where p enumerates the longitudinal TM waves, and r the transverse parts. The orthonormalization implies (though in our case of standing waves and time reversal symmetry all functions are real, we denote for generality the adjoint functions as in a complex function space)

$$\int \Psi_{s'}^\star(\vec{r})\Psi_s(\vec{r})d^3r=\delta_{s's},$$

and the boundary conditions are [see Eqs. (3) and (6)]

$$\chi_{rp}(x,y)|_S=0, \quad \left.\frac{d\psi_{TM,p}}{dz}\right|_{z=0,d}=0.$$

The eigenfunctions Ψ_s obey the eigenvalue equation

$$\left(\Delta+\frac{\omega_s^2}{c^2}\right)\Psi_s=0. \tag{22}$$

with eigenfrequencies ω_s, while the antenna wave functions have a continuous frequency spectrum

$$\left(\Delta+\frac{\omega^2}{c^2}\right)\Phi_\alpha=0. \tag{23}$$

From Eqs. (20), (22), and (23), we obtain

$$\frac{1}{c^2}(\omega^2-\omega_s^2)D_{\alpha s}=\int\{\Phi_\alpha^\star\Delta\Psi_s-\Psi_s^\star\Delta\Phi_\alpha\}d^3r. \tag{24}$$

Applying Green's theorem

$$\int (u\Delta v-v\Delta u)d^3r=\int\left(u\frac{\partial v}{\partial n}-v\frac{\partial u}{\partial n}\right)d\sigma,$$

we can convert the right side of Eq. (24) into a surface integral which has contributions from the surface S and from the horizontal plates $z=0$ and $z=d$:

$$\begin{aligned}\frac{1}{c^2}(\omega^2-\omega_s^2)D_{\alpha s}=&\int_S\left[\Phi_\alpha^\star\frac{\partial\Psi_s}{\partial n}-\Psi_s^\star\frac{\partial\Phi_\alpha}{\partial n}\right]d\sigma\\&+\int_{z=0}\left[\Phi_\alpha^\star\frac{\partial\Psi_s}{\partial n}-\Psi_s^\star\frac{\partial\Phi_\alpha}{\partial n}\right]d\sigma\\&+\int_{z=d}\left[\Phi_\alpha^\star\frac{\partial\Psi_s}{\partial n}-\Psi_s^\star\frac{\partial\Phi_\alpha}{\partial n}\right]d\sigma.\end{aligned} \tag{25}$$

The first integral vanishes, because on S both Φ_α and Ψ_s are zero according to the boundary conditions. The second integral also vanishes, since either $\partial\Psi_s/\partial n$ or $\partial\Phi_\alpha/\partial n$ is zero on the $(z=0)$ plane. The only nonvanishing contributions come from the third integral at each antenna footpoint ($\mu=\alpha,\ldots,N$). Because of the boundary conditions Eq. (16), we obtain

$$\begin{aligned}\frac{1}{c^2}(\omega^2-\omega_s^2)D_{\alpha s}&=-\sum_\mu\int_\mu\Psi_s^\star\frac{d\phi_{\alpha\mu}}{dz_\mu}|_0\chi_\mu(x_\mu,y_\mu)dxdy\\&=-\frac{1}{c}\left(\frac{\omega}{f\alpha}\right)^{1/2}f_{s\alpha}\psi_{TM,p}(d),\end{aligned}$$

$$f_{s\alpha}=\int_\alpha\chi_s^\star(x_\alpha,y_\alpha)\chi_\alpha(x_\alpha,y_\alpha)dx_\alpha dy_\alpha, \tag{26}$$

since only the antenna $\mu=\alpha$ contributes to the sum. From this we obtain for the expansion of Eq. (20)

$$\Phi_\alpha=c^2\sum_s\frac{1}{\omega_s^2-\omega^2}\frac{1}{c}\left(\frac{\omega}{f_\alpha}\right)^{1/2}f_{s\alpha}\Psi_s. \tag{27}$$

Contracting each side of Eq. (27) for an arbitrary antenna β with the transverse antenna wave $\chi_\beta^\star$ we obtain from Eq. (15), Eq. (27), and with $f_{s\beta}^\star = \int_\beta \chi_\beta^\star(x_\beta, y_\beta)\chi_s(x_\beta, y_\beta)dx_\beta dy_\beta$

$$\int_\beta \chi_\beta^\star \Phi_{\alpha\beta} dx_\beta dy_\beta = \mathcal{R}_{\alpha\beta}\frac{1}{c}\left(\frac{\omega}{f_\beta}\right)^{1/2}\int_\beta \chi_\beta^\star \chi_\beta dx_\beta dy_\beta$$

$$= \mathcal{R}_{\alpha\beta}\frac{1}{c}(\omega f_\beta)^{1/2}$$

$$= c^2 \sum_s \frac{1}{\omega_s^2 - \omega^2}\frac{1}{c}\left(\frac{\omega}{f_\alpha}\right)^{1/2} \times f_{s\alpha} f_{s\beta}^\star [\psi_{TM,s}(d)]^2. \quad (28)$$

With

$$\gamma_{s\mu} = \frac{c}{f_\mu^{1/2}} f_{s\mu}\psi_{TM,s}(d) \quad (29)$$

we finally get

$$\mathcal{R}_{\alpha\beta} = \sum_s \frac{\gamma_{s\alpha}\gamma_{s\beta}^\star}{\omega_s^2 - \omega^2}, \quad (30)$$

which is determined by the values of the cavity wave functions at the antenna footpoints. If one uses the proportionality of energy and frequency in quantum mechanics ($E = \hbar\omega$) the difference of the reactance matrix $\mathcal{R}$ in the electromagnetic and in the quantum case [1] is the resonance denominator. Here it contains the squares of the frequencies while in quantum mechanics the frequencies enter linearly.

The properties of the S matrix for time reversal invariant systems, unitarity and reciprocity, which lead to relations between the S-matrix elements that are not linearly independent, enter in a simple way into the $\mathcal{R}$ matrix: $\mathcal{R}$ is a real and symmetric matrix which (for N antennas) has $N(N+1)/2$ independent real parameters. Since for chaotic billiards one eventually wants to study systems that are not time reversal invariant, we have presented the derivation for the $\mathcal{R}$ matrix more generally, without using the reality condition.

III. THE EXPERIMENTAL RESONANCE SPECTRUM

As pointed out in Sec. II flat microwave cavities with cylindrical symmetry are a powerful tool for experimental studies of two-dimensional quantum billiards. While early experiments were carried out with normal conducting devices at room temperature [18,19], only superconducting resonators allow the measurement of complete spectra in a large frequency range with a high signal-to-noise ratio [10,11].

In [14] a chaotic billiard possessing threefold (C_3) symmetry was studied experimentally. Its spectrum shows single as well as double resonances (Fig. 3, upper part, and Figs. 4 and 5) and thus provides a basis to test resonance formulas for nondegenerate and nearly degenerate modes. The resonator used in the experiment is made from lead-plated copper and becomes superconducting below a critical temperature of $T_c = 7.2$ K. The height of the cavity is about 5.8 mm, and therefore two-dimensional wave propagation is ensured up to a critical frequency of about 25.5 GHz. The experiment was carried out inside a liquid helium cryostat under stable conditions, where at a temperature of 4.2 K the power transmitted from one antenna that emits microwaves to a second antenna that picks up microwaves was measured for frequencies from 45 MHz to 25 GHz in steps of 10 kHz. The antennas consist of a wire that penetrates the cavity through small holes in its lid by less than 0.5 mm. Due to the low rf resistance the superconducting resonator possesses a quality factor Q of the order of 10^5, and hence the lifted degeneracies of the double resonances can be resolved. Even higher quality factors ($Q \approx 10^7$) can be achieved when using electron-beam welded niobium resonators ($T_c = 9.2$ K) or three-

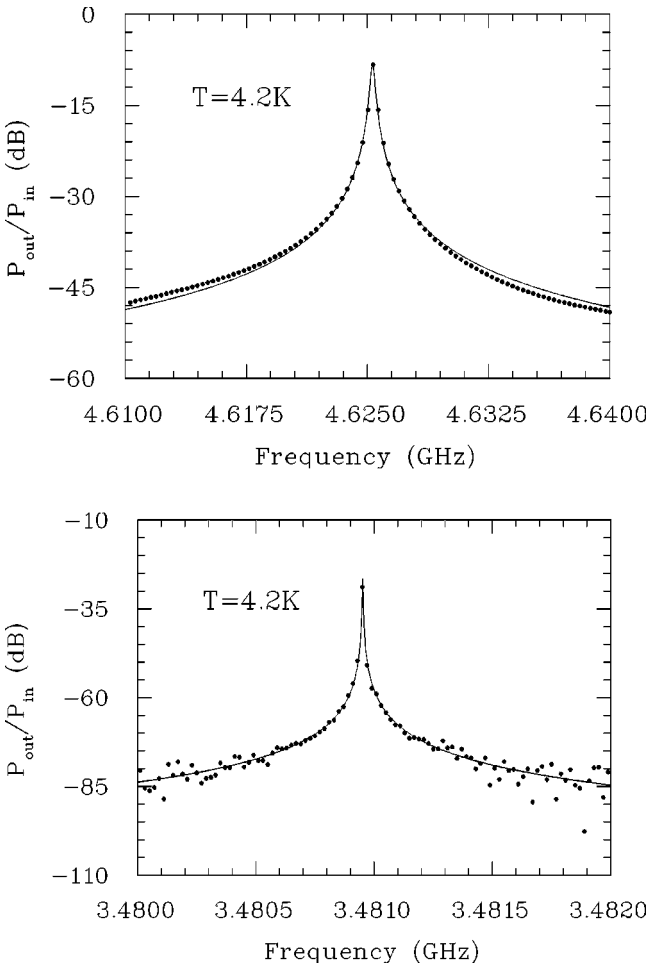

FIG. 3. Comparison of two resonances measured in superconducting resonators with different quality factors. Parameters of upper resonance (from [14], 2D lead resonator): $\Gamma_1/2\pi = 91.7$ kHz, $\Gamma_2/2\pi = 34.9$ kHz; $f_r = \omega_r/2\pi = 4.63$ GHz; $\lambda/2\pi = 84.1$ kHz; $\Gamma_{tot}/2\pi = 294.9$ kHz; $2\pi\tau = 11.9$ μs; fit accuracy $\chi^2 = 1.9$. Parameters of lower resonance (from [16], 3D niobium resonator): $\Gamma_1/2\pi = 0.02$ kHz, $\Gamma_2/2\pi = 0.18$ kHz; $f_r = \omega_r/2\pi = 3.48$ GHz; $\lambda/2\pi = 0.51$ kHz; $\Gamma_{tot}/2\pi = 1.22$ kHz; $2\pi\tau = 2.0$ ms; fit accuracy $\chi^2 = 9.7$.

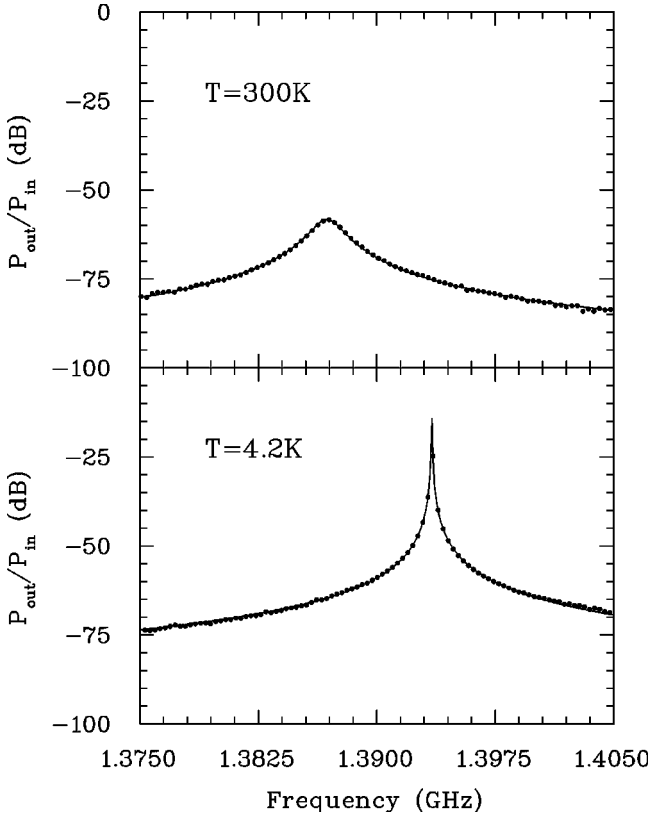

FIG. 4. Comparison of a "warm" ($T=300$ K) with a "cold" ($T=4.2$ K) cavity, showing the same isolated resonance in both cases. The shift of the resonance frequency is due to the reduction of the size of the cavity when cooling it to $T=4.2$ K. The fit curves coincide completely with the measured points. Parameters of upper resonance: $\Gamma_1/2\pi=1.3$ kHz, $\Gamma_2/2\pi=1.0$ kHz; $f_r=\omega_r/2\pi=1.387$ GHz; $\lambda/2\pi=949.2$ kHz; $\Gamma_{tot}/2\pi=1900.6$ kHz; $2\pi\tau=1.1$ μs; fit accuracy $\chi^2=1.07$. Parameters of lower resonance (from [14]): $\Gamma_1/2\pi=3.8$ kHz, $\Gamma_2/2\pi=4.0$ kHz; $f_r=\omega_r/2\pi=1.393$ GHz; $\lambda/2\pi=10.3$ kHz; $\Gamma_{tot}/2\pi=28.4$ kHz; $2\pi\tau=91.1$ μs; fit accuracy $\chi^2=0.6$.

dimensional microwave billiards (see [11]). The latter, however, do not show an analogy between the Helmholtz and Schrödinger equations or cylindrical symmetry, but the wave chaotic phenomena of the vectorial Helmholtz equation. Such a billiard was studied in [16] and we analyzed some of its resonances here for comparison (Fig. 3, lower part, and Fig. 6).

For our analyses we chose resonances in the low and high frequency parts of the spectra (Figs. 3, 4, 5, and 6). We also measured one single resonance of the C_3 billiard at room temperature, i.e., with the normal conducting resonator. This clearly shows a broader resonance line and a reduction of the power transmitted by several orders of magnitude (Fig. 4). A more detailed description of experiments with superconducting microwave billiards can be found in [11]. It should be emphasized, however, that, although the measurement of a whole spectrum typically takes one or more days, the data points in the vicinity of an individual resonance are taken within a few seconds under identical circumstances. This ensures the high precision of our experimental resonance lines.

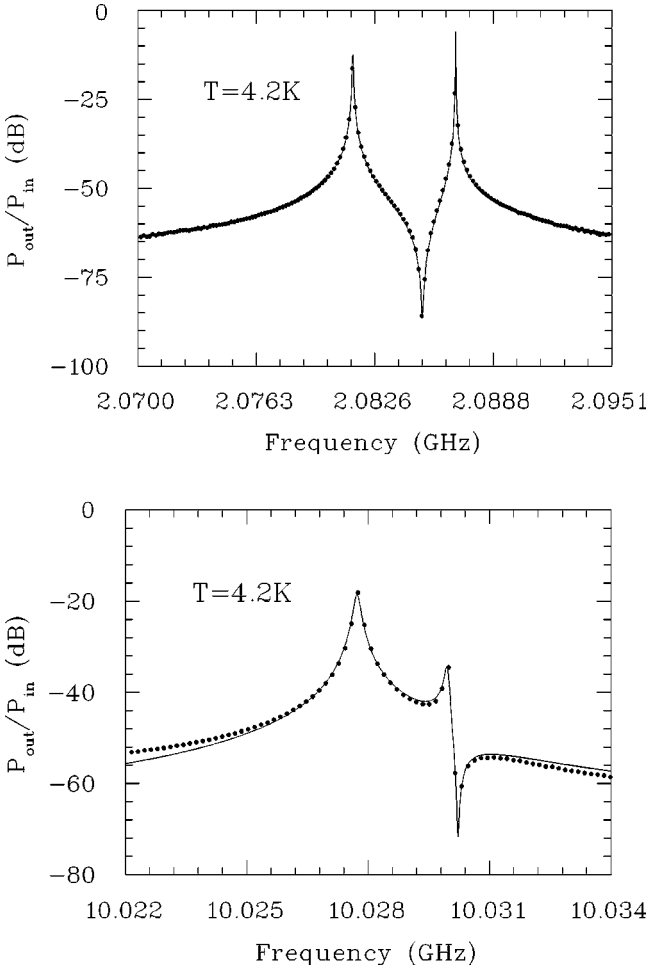

FIG. 5. Two interfering double resonances (from [14]). Parameters of upper resonance, first resonance: $\Gamma_{11}/2\pi=6.5$ kHz, $\Gamma_{12}/2\pi=4.7$ kHz; $f_{1r}=\omega_{1r}/2\pi=2.081$ GHz; $\lambda_1/2\pi=14.0$ kHz; $\Gamma_{1,tot}/2\pi=39.1$ kHz; $2\pi\tau_1=71.4$ μs; second resonance: $\Gamma_{21}/2\pi=3.0$ kHz, $\Gamma_{22}/2\pi=2.3$ kHz; $f_{2r}=\omega_{2r}/2\pi=2.087$ GHz; $\lambda_2/2\pi=4.8$ kHz; $\Gamma_{2,tot}/2\pi=14.9$ kHz; $2\pi\tau_2=209.9$ μs; fit accuracy $\chi^2=0.67$. Parameters of lower resonance, first resonance: $\Gamma_{11}/2\pi=10.5$ kHz, $\Gamma_{12}/2\pi=9.9$ kHz; $f_{1r}=\omega_{1r}/2\pi=10.028$ GHz; $\lambda_1/2\pi=74.8$ kHz; $\Gamma_{1,tot}/2\pi=170.0$ kHz; $2\pi\tau_1=13.4$ μs; second resonance: $\Gamma_{21}/2\pi=0.0033$ kHz, $\Gamma_{22}/2\pi=34.7$ kHz; $f_{2r}=\omega_{2r}/2\pi=10.030$ GHz; $\lambda_2/2\pi=29.7$ kHz; $\Gamma_{2,tot}/2\pi=94.1$ kHz; $2\pi\tau_2=33.7$ μs; fit accuracy $\chi^2=3.0$.

IV. ANALYSIS OF SINGLE AND DOUBLE RESONANCES

For the analysis of experimentally determined resonances we augment the $\mathcal{R}$ matrix Eq. (30) in two respects. First, we allow for the fact that the superconducting cavity is not a perfect conductor for electromagnetic waves. This results in an overall damping of the fields, which are no longer strictly harmonic, as assumed in Eq. (1). We account for this by adding to the frequency a small imaginary part, $\omega_s \rightarrow \omega_s - i\lambda_s$, which results in an additional broadening of the resonances (cf. [17], Chap. 8.8, where cavity losses because of finite wall conductivity are treated explicitly).

The introduction of a damping factor λ produces a redundance problem for the extraction of the resonance parameters from the fitted spectra. Since the $\mathcal{R}$ matrix contains for two

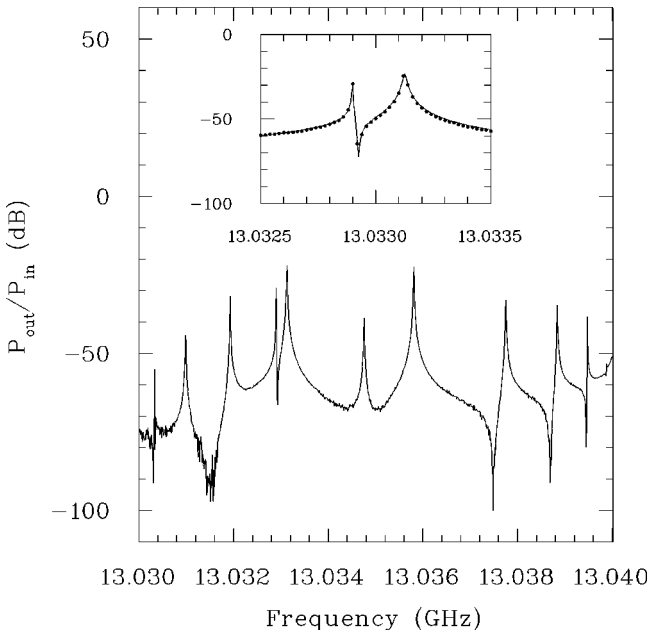

FIG. 6. Part of the transmission spectrum of a 3D stadium billiard [16] in the vicinity of 13.03 GHz, where the resonances can still be described with the fit formulas. Fit parameters for the double resonance shown in the inset, first resonance: $\Gamma_{11}/2\pi=0.550$ kHz, $\Gamma_{12}/2\pi=0.008$ kHz; $f_{1r}=\omega_{1r}/2\pi=13.0329$ GHz; $\lambda_1/2\pi=1.44$ kHz; $\Gamma_{1,tot}/2\pi=2.889$ kHz; second resonance: $\Gamma_{21}/2\pi=0.528$ kHz; $\Gamma_{22}/2\pi=0.529$ kHz, $f_{2r}=\omega_{2r}/2\pi=13.0331$ GHz, $\lambda_2/2\pi=7.16$ kHz, $\Gamma_{2,tot}/2\pi=14.32$ kHz; fit accuracy $\chi^2=1.1$.

antennas and s overlapping resonances $3s$ independent parameters (the reduced widths $\gamma_{s1,s2}$ and resonance frequencies ω_s), we introduce s parameters more, the damping factors λ_s. This overdetermines the analysis since one can shift in the parameter space between the partial widths $\Gamma_{si}=\gamma_{si}^2$ determining the resonance strengths and widths and the damping factors λ_s, without changing the fit. We have carefully analyzed this problem analytically and numerically. The result is that the uncertainty introduced thereby does not influence the leading order of the partial widths and damping factors.

For the numerical analysis we set $c=1$, which then measures the wave numbers k_μ and the γ_μ in s^{-1}.

A. Single resonances

For single resonances the power transfer between one input and one output antenna, $P_{12}=|S_{12}|^2$, is determined by Eq. (12) and Eq. (17), which connect the reactance matrix with the S matrix. For a single resonance, viz., only one term in Eq. (30), this leads to a resonance formula that resembles in its structure the Lorentz line (for the relation between this and the Breit-Wigner form, see Sec. V)

$$P_{12}(\omega)=\frac{4\gamma_1^2k_1\gamma_2^2k_2}{(\omega^2-\omega_r^2+\lambda^2)^2+(\gamma_1^2k_1+\gamma_2^2k_2+2\lambda\omega_r)^2}, \tag{31}$$

where in the one-level evaluation of Eq. (30) the index $s=1$ has been omitted. The partial widths Γ_i and the additional damping factor ϵ are (the reason for this choice is presented in Sec. V)

$$\Gamma_i=\gamma_i^2, \quad \epsilon=2\lambda, \tag{32}$$

which results in the total width

$$\Gamma_{tot}=\Gamma_1+\Gamma_2+\epsilon, \tag{33}$$

and the lifetime of the resonance is given with the complex resonance frequency as $\tau=\lambda^{-1}$.

The evaluation of the parameters in Eq. (31) for a given cavity resonance is performed with the software package MATHEMATICA 4.1, ''Nonlinear Fit.'' For the antenna wave numbers k_i we use the common value $k_i=\omega(i=1,2)$, which is the dominant mode for a coaxial cable [17].

Figure 3 shows two isolated cavity resonances (dotted points) and their analysis with the theoretical relation Eq. (31) (continuous line). The fit to the experimental points over a total interval of four to seven orders of magnitude is nearly perfect, and this shows the reliability of the derived resonance formula. The resonance parameters are listed in the figure caption.

Figure 4 depicts the comparison of an isolated resonance in a ''warm,'' normally conducting cavity with the same resonance in the superconducting cavity. The drastic increase of the width is due to the additional wall damping. In the analysis this is reflected in the vastly increased damping factor ϵ. There is also a shift of the resonance frequency, because the superconducting cavity at $T=4.2$ K is contracted in size, and thus its eigenfrequencies are higher (cf. [18–20]). For the resonance parameters, see the figure caption.

B. Double resonances

In this case the $\mathcal{R}$ matrix is given by [see Eq. (30)]

$$\mathcal{R}_{12}=\frac{\gamma_{11}\gamma_{12}}{\omega_1^2-\omega^2}+\frac{\gamma_{21}\gamma_{22}}{\omega_2^2-\omega^2}. \tag{34}$$

The resulting expression for the S matrix, Eq. (17), is extremely involved, containing a lot of nonlinear interference terms, and it cannot be simplified since no small parameter for an expansion can be defined. So we present the resulting formula for P_{12} only in the Appendix. It is obtained by inserting Eq. (34) into Eq. (17), and this into Eq. (12). Figure 5 shows two interfering double resonances and their analysis in $\mathcal{R}$-matrix theory. The two resonances exhibit very different interference structures which are both well described by the $\mathcal{R}$-matrix approach. The resonance parameters for both resonances are again listed in the figure caption, where the individual parameters for the two resonances have restricted significance because of the strong interference between them.

In Fig. 6 we present a section of the high frequency part of the spectrum of the three-dimensional 3D-cavity (from Ref. [16], there are more than 5000 resonances below this section). It can be seen that the resonances are still well separated, leading to single and at most double resonances. The inset presents a fit to the double resonance around

13.033 GHz and shows the applicability of our analysis also in this part of the spectrum of a cavity which is not of a cylindrical symmetric shape.

In all the analyses shown, the quoted fit accuracy χ^2 refers to the performed logarithmic fit of the logarithmic data.

V. COMPARISON OF THE CAVITY RESONANCE WITH THE BREIT-WIGNER FORMULA

For the comparison of the two one-level formulas we start from Eq. (31), i.e.,

$$P_{12}(\omega)=\frac{4\gamma_1^2k_1\gamma_2^2k_2}{(\omega^2-\omega_r^2+\lambda^2)^2+(\gamma_1^2k_1+\gamma_2^2k_2+2\lambda\omega_r)^2}.$$

With $k_1=k_2=\omega$ and $\omega_{eff}^2:=\omega_r^2-\lambda^2$, one obtains

$$P_{12}(\omega)=\frac{4\gamma_1^2\gamma_2^2\omega^2}{(\omega-\omega_{eff})^2(\omega+\omega_{eff})^2+(2\lambda\omega_r+\gamma_1^2\omega+\gamma_2^2\omega)^2}. \tag{35}$$

For narrow resonances $\Gamma,\lambda\ll\omega_r$ the response is nonvanishing only around $\omega\approx\omega_r$. Then we can set

$$\omega=\omega_{eff}+\delta_1\omega,\quad \omega=\omega_r+\delta_2\omega,\quad \text{and}\quad \frac{\delta_1\omega}{\omega_r},\frac{\delta_2\omega}{\omega_r}\ll 1.$$

Up to first order in $\delta_1\omega/\omega$ and $\delta_2\omega/\omega$, Eq. (35) takes the form

$$P_{12}(\omega)\approx\frac{\gamma_1^2\gamma_2^2}{(\omega-\omega_{eff})^2(1-\delta_1\omega/2\omega)^2+\frac{1}{4}[2\lambda(1-\delta_2\omega/\omega)+\gamma_1^2+\gamma_2^2]^2}.$$

Neglecting the small corrections $\delta_1\omega/\omega,\delta_2\omega/\omega$, and with the partial and total widths of Eqs. (32) and (33), $P_{12}(\omega)$ assumes the Breit-Wigner form

$$P_{12}(\omega)\approx\frac{\Gamma_1\Gamma_2}{(\omega-\omega_{eff})^2+\left(\frac{1}{2}\Gamma_{tot}\right)^2}. \tag{36}$$

To give an example, for the first resonance of Fig. 3 we have $\Gamma_{tot}/2\pi=294.9$ kHz, $f_r=\omega_r/2\pi=4.63$ GHz, and thus, with $\delta\omega\approx\Gamma_{tot}$, $\Gamma_{tot}/\omega_r=6.5\times10^{-5}$. Consequently, the Breit-Wigner formula is an excellent approximation for narrow single resonances in the electromagnetic case.

VI. CONCLUSION

In this paper we study the resonance spectrum of a flat electromagnetic resonance cavity which is fed through an input antenna and analyzed by one or several output antennas. The TM eigenstates of the cavity obey the same Helmholtz eigenvalue equation as the two-dimensional stationary quantum problem in the same geometry (quantum billiard). Thus the study of cavity resonances provides, especially in the almost lossless superconducting case, an excellent tool to study experimentally the spectral properties of regular and chaotic quantum billiards. It is therefore of great importance for the analysis of the electromagnetic case to derive a reliable resonance formula which not only reproduces the resonance shapes, but from which one can also deduce the relevant resonance parameters.

We derive the cavity resonance formula in close analogy to the Wigner-Eisenbud $\mathcal{R}$-matrix theory, which is a cornerstone in nuclear reaction theory and has been used in various fields, especially recently in atomic physics in the analysis of Rydberg atoms and multiphoton ionization. The goal of this approach is to express the S matrix in terms of properties of the wave function at the channel entrances, which in our case are the antenna footpoints at the cavity. We succeed in expressing the cavity-antenna couplings in terms of the cavity eigenfunctions at the antenna entrances. As in the nuclear case, the resonance parameters can then be extracted by fitting measured resonance shapes. Differences from the nuclear case come from the different dispersion laws of the electromagnetic and quantum cases, and from the geometrical properties of TM resonances in the flat cylindrical cavity. For single, narrow resonances, however, the usual Breit-Wigner formula is an excellent approximation to the electromagnetic Lorentz line shape.

We apply our multiantenna result to measured well resolved single and double resonances of a superconducting cavity with one input and one output antenna. The fits are almost perfect over many orders of magnitude of the transmitted power. Rather involved interference patterns of double resonances (see Fig. 5) are well accounted for by the two-level formula, even in the high frequency parts of the spectra.

ACKNOWLEDGMENTS

We thank H.-D. Gräf for his ideas and suggestions concerning the experiments. C.D., A.H., and A.R. thank H. L. Harney for valuable remarks concerning the numerical evaluation of the resonance formulas. This work was supported by the DFG under Contract No. Ri 242/16-3.

APPENDIX: THE FIT FORMULA FOR TWO ANTENNAS IN THE TWO-LEVEL CASE

The power transfer P_{12} from the input to the output antenna is determined according to Eq. (12) by the absolute

square of the S-matrix element:

$$P_{12}=\frac{P_{12}^{out}}{P_1^{in}}=|S_{12}|^2. \tag{A1}$$

The S matrix is given according to Eq. (17) as

$$S=\rho(1-iB\mathcal{R}B)^{-1}(1+iB\mathcal{R}B)\rho. \tag{A2}$$

Since the diagonal phase factor ρ does not contribute to the absolute square, we omit it in the following. Then we obtain with $B\mathcal{R}B\equiv M$

$$S_{12}(\omega)=\frac{2iM_{12}(\omega)}{1-iM_{11}(\omega)+M_{12}(\omega)M_{21}(\omega)-iM_{22}(\omega)-M_{11}(\omega)M_{22}(\omega)}. \tag{A3}$$

In order to simplify the evaluation we absorb the diagonal B matrix in the partial widths γ_B, and with $k_i=\omega$ (cf. Sec. VI) we set

$$\gamma_{B,ij}(\omega)=\sqrt{\omega}\gamma_{ij} \quad (i,j)=(1,2). \tag{A4}$$

Now we obtain from Eq. (34) for $B\mathcal{R}B$

$$M_{i,j}=\frac{\gamma_{B,1i}\gamma_{B,1j}}{\omega_1^2-\omega^2}+\frac{\gamma_{B,2i}\gamma_{B,2j}}{\omega_2^2-\omega^2}, \tag{A5}$$

and, as pointed out in Sec. VI, a small imaginary part is added to the frequencies:

$$\omega_1=\omega_{1r}-i\lambda_1, \quad \omega_2=\omega_{2r}-i\lambda_2.$$

Inserting Eq. (A5) into Eq. (A3) and taking the absolute square $S^\star S$, one arrives at the extremely involved result for P_{12}, Eq. (A1), for interfering double resonances. For time reversal invariant systems, which we analyze in this paper exclusively, one obtains

$$P_{12}(\omega)=\frac{N(\omega)}{D(\omega)}$$

with

$$N(\omega)=4\{[2\gamma_{B,21}\gamma_{B,22}\lambda_1\omega_{1,r}+2\gamma_{B,11}\gamma_{B,12}\lambda_2\omega_{2,r}]^2+[\gamma_{B,21}\gamma_{B,22}(\lambda_1^2+\omega^2-\omega_{1,r}^2)+\gamma_{B,11}\gamma_{B,12}(\lambda_2^2+\omega^2-\omega_{2,r}^2)]^2\}^2, \tag{A6}$$

$$\begin{aligned}D(\omega)=&[\lambda_2^2(\gamma_{B,11}^2+\gamma_{B,12}^2+2\lambda_1\lambda_2^2\omega_{1,r})+(\gamma_{B,11}^2+\gamma_{B,12}^2)\omega^2+2\lambda_1\omega^2\omega_{1,r}+(\gamma_{B,21}^2+\gamma_{B,22}^2)(\lambda_1^2+\omega^2-\omega_{1,r}^2)\\&+2\lambda_2(\lambda_1^2\omega_{2,r}+\omega^2\omega_{2,r}-\omega_{1,r}^2\omega_{2,r})-(\gamma_{B,11}^2+\gamma_{B,12}^2)\omega_{2,r}^2-2\lambda_1\omega_{1,r}\omega_{2,r}^2]^2[\gamma_{B,11}^2\gamma_{B,21}^2-2\gamma_{B,11}\gamma_{B,12}\gamma_{B,21}\gamma_{B,22}\\&+\gamma_{B,11}^2\gamma_{B,22}^2-\lambda_1^2\lambda_2^2-(\lambda_1^2+\lambda_2^2)\omega^2-\omega^4+2(\gamma_{B,21}^2+\gamma_{B,22}^2)\lambda_1\omega_{1,r}+\lambda_2^2\omega_{1,r}^2+\omega^2\omega_{1,r}^2+2\gamma_{B,11}^2\lambda 2\omega_{2,r}\\&+2\gamma_{B,12}^2\lambda_2\omega_{2,r}+4\lambda_1\lambda_2\omega_{1,r}\omega_{2,r}+(\lambda_1^2+\omega^2-\omega_{1,r}^2)\omega_{2,r}^2]^2.\end{aligned} \tag{A7}$$

Setting $\gamma_{B,21}=\gamma_{B,22}=\lambda_2=\omega_{2,r}=0$ and dividing numerator and denominator by ω^4, one obtains the single resonance formula of Eq. (31).

In the parameter search of the fitting procedure one has to assure that the decay parameters λ_1,λ_2 stay positive. This can be achieved by setting $\lambda_i=(\lambda_i^2)^{(1/2)}$.

[1]

[1] E.P. Wigner and L. Eisenbud, Phys. Rev. **72**, 29 (1947).
[2] P.L. Kapur and R. Peierls, Proc. R. Soc. London, Ser. A **166**, 277 (1938).
[3] A.M. Lane and R.G. Thomas, Rev. Mod. Phys. **30**, 257 (1958).
[4] P.G. Burke, P. Francken, and C.J. Joachain, J. Phys. B **24**, 761 (1991).
[5] J. Purvis, M. Dörr, M. Terao-Dunseath, C.J. Joachain, P.G. Burke, and C.J. Noble, Phys. Rev. Lett. **71**, 3943 (1993).
[6] M.H. Halley, D. Delande, and K.T. Taylor, J. Phys. B **26**, 1775 (1993).
[7] G.D. Stevens, C.-H. Iu, T. Bergeman, H.J. Metcalf, I. Seipp, K.T. Taylor, and D. Delande, Phys. Rev. A **53**, 1349 (1996).
[8] A. Krug and A. Buchleitner, Europhys. Lett. **49**, 176 (2000).
[9] A. Krug and A. Buchleitner, Phys. Rev. Lett. **86**, 3538 (2001).
[10] H.-D. Gräf, H.L. Harney, H. Lengeler, C.H. Lewenkopf, C. Rangacharyulu, A. Richter, P. Schardt, and H.A. Weidenmüller, Phys. Rev. Lett. **69**, 1296 (1992).
[11] A. Richter, in *Emerging Applications of Number Theory*, edited by D.A. Hejhal, J. Friedman, M.C. Gutzwiller, and A.M. Odlyzko, IMA Volumes in Mathematics and its Applications Vol. 109 (Springer, New York, 1999), pp. 479–523.
[12] H. Alt, P. von Brentano, H.-D. Gräf, R.-D. Herzberg,

M. Philipp, A. Richter, and P. Schardt, Nucl. Phys. A **560**, 293 (1993).

[13] H. Alt, P. von Brentano, H.-D. Gräf, R. Hofferbert, M. Philipp, H. Rehfeld, A. Richter, and P. Schardt, Phys. Lett. B **366**, 7 (1996).

[14] C. Dembowski, H.-D. Gräf, A. Heine, H. Rehfeld, A. Richter, and C. Schmit, Phys. Rev. E **62**, R4516 (2000).

[15] C. Dembowski, B. Dietz, H.-D. Gräf, A. Heine, F. Leyvraz, M. Miski-Oglu, A. Richter, and T.H. Seligman, Phys. Rev. Lett. **90**, 014102 (2003).

[16] C. Dembowski, B. Dietz, H.-D. Gräf, A. Heine, T. Papenbrock, A. Richter, and C. Richter, Phys. Rev. Lett. **89**, 064101 (2002).

[17] J.D. Jackson, *Classical Electrodynamics*, 2nd ed. (Wiley, New York, 1975), Chap. 8.

[18] H.-J. Stöckmann and J. Stein, Phys. Rev. Lett. **64**, 2215 (1990).

[19] S. Sridhar, Phys. Rev. Lett. **67**, 785 (1991).

[20] H. Alt, C. Dembowski, H.-D. Gräf, R. Hofferbert, H. Rehfeld, A. Richter, R. Schuhmann, and T. Weiland, Phys. Rev. Lett. **79**, 1026 (1997).